Thermally Cross-Linkable Hole-Transporting Materials for Improving Hole Injection in Multilayer Blue-Emitting Phosphorescent Polymer Light-Emitting Diodes

ARTICLE *in* MACROMOLECULES · NOVEMBER 2008

Impact Factor: 5.8 · DOI: 10.1021/ma801374w

8 AUTHORS, INCLUDING:

Hin-Lap Yip
South China University of Technology
125 PUBLICATIONS **6,880** CITATIONS
SEE PROFILE

Jingdong Luo
University of Washington Seattle
260 PUBLICATIONS **7,379** CITATIONS
SEE PROFILE

Alex K-Y Jen
University of Washington Seattle
391 PUBLICATIONS **15,943** CITATIONS
SEE PROFILE

Thermally Cross-Linkable Hole-Transporting Materials on Conducting Polymer: Synthesis, Characterization, and Applications for Polymer Light-Emitting Devices

Yen-Ju Cheng,[†] Michelle S. Liu,[†] Yong Zhang,[†] Yuhua Niu,[†] Fei Huang,[†,‡] Jae-Won Ka,[†] Hin-Lap Yip,[†,‡] Yanqing Tian,[†,‡] and Alex K.-Y. Jen*[,†,‡]

Department of Materials Sciences & Engineering and Institute of Advanced Materials and Technology, University of Washington, Seattle, Washington 98195

Received July 11, 2007. Revised Manuscript Received November 29, 2007

A series of novel hole-transporting materials (HTMs) bearing thermally cross-linkable styryl groups have been synthesized and characterized. These HTMs could be *in situ* cross-linked under mild thermal polymerization without any initiator. The cross-linking temperatures (150–180 °C) for these HTMs are substantially lower than that typically used for curing perfluorocyclobutane (PFCB)-based HTMs (230 °C). After cross-linking, the resultant HTMs form robust, smooth, and solvent-resistant networks, which enables the subsequent spin-coating of emissive layer (EML). The HTMs based on an ether linkage connecting triarylamine dimers exhibited better hole-transporting ability compared to their corresponding monotriarylamine compounds due to higher content and closer distance of the hole-transporting units. Most importantly, the milder cross-linking condition for these HTMs allows the commonly used conducting polymer, poly(3,4-ethylenedioxythiophene):poly(4-styrenesulfonate) (PEDOT:PSS), to be incorporated as the bottom hole-injecting layer to improve turn-on voltage and power efficiency of the devices. This PEDOT/HTM double-layer hole-injecting/hole-transporting configuration also provides the combined advantages of preventing acidic PEDOT:PSS-induced quenching of emission, facilitating cascade hole injection and transport, and functioning as an efficient electron blocker. One of the devices that combines 2-NPD with PEDOT:PSS showed much improved performance of low turn-on voltage (3.3 V), high luminous efficiency (10.8 cd/A), and brightness (21 500 cd/m^2).

Introduction

Organic and polymer light-emitting diodes (LEDs) have been the subject of intensive research due to their potential applications in solid-state lighting and flat-panel displays. To achieve high-performance LEDs devices, charge injection and transport from both the anode and the cathode must be balanced to yield the optimal formation of excitons.[1] These requirements can be fulfilled by using multilayer architectures with discrete hole-transporting layer (HTL), light-emitting layer (EML), and electron-transporting layer (ETL) sandwiched between two electrodes. Such configurations allow each layer of material to be optimized individually for charge injection, transport, and emission. For small-molecule-based LEDs, it is straightforward to realize well-defined multilayer structures through layer-by-layer vacuum deposition. For polymer-based LEDs, multilayer configuration can be achieved by either spin-coating or inject printing which has some advantages over the vapor evaporation method for lower cost and large-area coating. However, one of the major challenges for solution processing is the erosion of bottom layer caused by solvent used in the subsequent step. To alleviate this problem, the utilization of self-assembled layer[2] or orthogonal solvents[3] for processing has been reported. In addition, there is a variety of thermally,[4] photochemically,[5] and electro-

* To whom correspondence should be addressed.
[†] Department of Materials Sciences & Engineering.
[‡] Institute of Advanced Materials and Technology.

(1) (a) Strukelj, M.; Papadimitrakopoulos, F.; Miller, T. M.; Rothberg, L. J. *Science* **1995**, *267*, 1969. (b) Burroughes, J. H.; Bradley, D. D. C.; Brown, A. R.; Marks, R. N.; Mackay, K.; Friend, R. H.; Burns, P. L.; Holmes, A. B. *Nature (London)* **1990**, *347*, 539.

(2) (a) Ho, P. K. H.; Granström, M.; Friend, R. H.; Greenham, N. C. *Adv. Mater.* **1998**, *10*, 769. (b) Ho, P. K. H.; Kim, J.-S.; Burroughes, J. H.; Becker, H.; Li, S. F. Y.; Brown, T. M.; Cacialli, F.; Friend, R. H. *Nature (London)* **2000**, *404*, 481. (c) Huang, Q.; Evmenenko, G. A.; Dutta, P.; Lee, P.; Armstrong, N. R.; Marks, T. J. *J. Am. Chem. Soc.* **2005**, *127*, 10227. (d) Veinot, J. G. C.; Marks, T. J. *Acc. Chem. Res.* **2005**, *38*, 632. (e) Lee, J.; Jung, B.-J.; Lee, J.-I.; Chu, H. Y.; Do, L.-M.; Shim, H.-K. *J. Mater. Chem.* **2002**, *12*, 3494.

(3) (a) Gong, X.; Wang, S.; Moses, D.; Bazan, G. C.; Heeger, A. J. *Adv. Mater.* **2005**, *17*, 2053. (b) Ma, W.; Iyer, P. K.; Gong, X.; Liu, B.; Moses, D.; Bazan, G. C.; Heeger, A. J. *Adv. Mater.* **2005**, *17*, 274. (c) Huang, F.; Hou, L.; Wu, H.; Wang, X.; Shen, H.; Cao, W.; Yang, W.; Cao, Y. *J. Am. Chem. Soc.* **2004**, *126*, 9845. (d) Wu, H.; Huang, F.; Mo, Y.; Yang, W.; Wang, D.; Peng, J.; Cao, Y *Adv. Mater.* **2004**, *16*, 1826.

(4) (a) Zhao, J.; Bardecker, J. A.; Munro, A. M.; Liu, M. S.; Niu, Y.; Ding, I.-K.; Luo, J.; Chen, B.; Jen, A. K.-Y.; Ginger, D. S. *Nano Lett.* **2006**, *6*, 462. (b) Liu, S.; Jiang, X.; Ma, H.; M. Liu, S.; Jen, A. K.-Y. *Macromolecules* **2000**, *33*, 3514. (c) Jiang, X.; Liu, S.; Liu, M. S.; Herguth, P.; Jen, A. K.-Y.; Fong, H.; Sarikaya, M. *Adv. Funct. Mater.* **2002**, *12*, 745. (d) Niu, Y.; Liu, M. S.; Ka, J.-W.; Jen, A. K.-Y. *Appl. Phys. Lett.* **2006**, *88*, 093505. (e) Lim, B.; Hwang, J.-T.; Kim, J. Y.; Ghim, J.; Vak, D.; Noh, Y.-Y.; Lee, S.-H.; Lee, K.; Heeger, A. J.; Kim, D.-Y. *Org. Lett.* **2006**, *8*, 4703. (f) Li, W.; Wang, Q.; Cui, J.; Chou, H.; Shaheen, S. E.; Jabbour, G. E.; Anderson, J.; Lee, P.; Kippelen, B.; Peyghambarian, N.; Armstrong, N. R.; Marks, T. J. *Adv. Mater.* **1999**, *11*, 730. (g) Paul, G. K.; Mwaura, J.; Argun, A. A.; Taranekar, P.; Reynolds, J. R. *Macromolecules* **2006**, *39*, 7789. (h) Niu, Y.-H.; Liu, M. S.; Ka, J.-W.; Bardeker, J.; Zin, M. T.; Schofield, R.; Chi, Y.; Jen, A. K.-Y. *Adv. Mater.* **2007**, *19*, 300. (i) Niu, Y.-H.; Munro, A. M.; Cheng, Y.-J.; Tian, Y.; Liu, M. S.; Zhao, J.; Bardecker, J. A.; Plante, I. J.-L.; Ginger, D. S.; Jen, K.-Y. *Adv. Mater.* **2007**, *19*, 3371.

10.1021/cm071828o CCC: $40.75
Published on Web 12/29/2007

chemically[6] cross-linkable materials that can be used to overcome the interfacial mixing caused by solution processing. These small-molecule-based HTMs can be *in situ* converted into solvent-resistant, cross-linked networks. This provides an ideal solution to avoid tedious synthesis and purification that are often encountered for polymers. Higher purity HTMs obtained from this approach also enables better reproducibility of device results. Moreover, it provides better morphological stability[7] and reduced crystallization[8] which are the main problems frequently occurred in small-molecule-based HTMs. Previously, we have reported the development of perfluorocyclobutane (PFCB) aryl ether HTMs based on thermal cross-linking of trifluorovinylphenyl ether group.[4a–e,9] Although light-emitting devices made from these HTMs have been shown to have improved device performance, the required condition for high curing temperature (>225 °C) and long duration (1–2 h) to complete the reaction is very harsh. This often poses limitation on the choice of other device components to be used. The commonly used conducting polymer, PEDOT:PSS, is a good hole-injection material due to its good electrical and mechanical properties.[10] By forming a HT layer on PEDOT:PSS, it provides an ideal path for cascade hole injection for improving device performance.[11] It also leads to reduced turn-on voltage and longer device lifetime.[12] Moreover, inserting a HTM interlayer between PEDOT:PSS and the emissive layer prevents quenching of excitons at the adjacent PEDOT:PSS interface[13] and provides effective electron blocking.[14] However, the prolonged high-temperature curing for the upper HTM tends to degrade PEDOT:PSS because of the decomposition of sulfonic acids in PSS[15] or etching of the ITO.[16] Therefore, it is desirable to find a way to reduce curing temperature and time of the top layer HTM. It was reported that styrene undergoes rapid polymerization to form polystyrene by heating without any initiators.[17] From the practical point of view, the styryl group is a promising thermal curable group because it can be polymerized at lower temperature and is much easier to synthesize.[18] The chemical structures of HTMs used in this study are shown in Scheme 1.

Scheme 1. Chemical Structures of HTMs

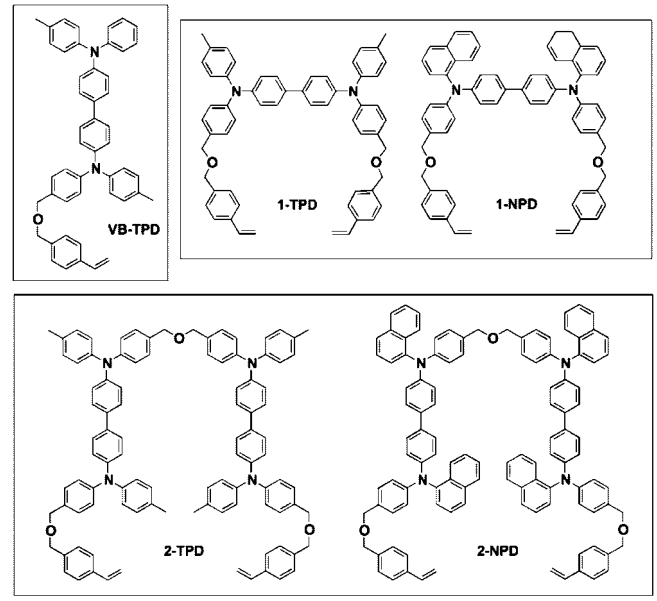

N,*N*′-Bis(tolyl)-*N*,*N*′-diphenyl-1,1′-biphenyl-4,4′-diamine (TPD) and *N*,*N*′-bis(1-naphthyl)-*N*,*N*′-diphenyl-1,1′-biphenyl-4,4′-diamine (NPD), two of the most commonly used HTMs,[19] are functionalized with two styryl groups for thermal cross-linking (1-TPD and 1-NPD). It was reported that by substituting the ester linkage with less polar ether group and connecting the HTMs with shorter linker tend to enhance the device performance.[5e] Therefore, the shortest dimethylene ether group (−CH_2−O−CH_2−) was employed

(5) (a) Bacher, E.; Bayerl, M.; Rudati, P.; Reckefuss, N.; Müller, C. D.; Meerholz, K.; Nuyken, O. *Macromolecules* **2005**, *38*, 1640. (b) Müller, C. D.; Falcou, A.; Reckefuss, N.; Rojahn, M.; Wiederhirn, V.; Rudati, P.; Frohne, H.; Nuyken, O.; Becker, H.; Meerholz, K. *Nature (London)* **2003**, *421*, 829. (c) Domercq, B.; Hreha, R. D.; Zhang, Y.-D.; Larribeau, N.; Haddock, J. N.; Schultz, C.; Marder, S. R.; Kippelen, B. *Chem. Mater.* **2003**, *15*, 1491. (d) Zhang, Y.-D.; Hreha, R. D.; Jabbour, G. E.; Kippelen, B.; Peyghambarian, N.; Marder, S. R. *J. Mater. Chem.* **2002**, *12*, 1703. (e) Bellmann, E.; Shaheen, S. E.; Thayumanavan, S.; Barlow, S.; Grubbs, R. H.; Marder, S. R.; Kippelen, B.; Peyghambarian, N. *Chem. Mater.* **1998**, *10*, 1668. (f) Bacher, A.; Erdelen, C. H.; Paulus, W.; Ringsdorf, H.; Schmidt, H.-W.; Schuhmacher, P. *Macromolecules* **1999**, *32*, 4551. (g) Yang, X.; Müller, D. C.; Neher, D.; Meerholz, K. *Adv. Mater.* **2006**, *18*, 948.

(6) (a) Xia, C.; Advincula, R. C. *Chem. Mater.* **2001**, *13*, 1682. (b) Baba, A.; Onishi, K.; Knoll, W.; Advincula, R. C. *J. Phys. Chem. B* **2004**, *108*, 18949. (c) Inaoka, S.; Roitman, D. B.; Advincula, R. C. *Chem. Mater.* **2005**, *17*, 6781. (d) Chou, M.-Y.; Leung, M.-K.; Su, Y. O.; Chiang, C. L.; Lin, C.-C.; Liu, J.-H.; Kuo, C.-K.; Mou, C.-Y. *Chem. Mater.* **2004**, *16*, 654.

(7) (a) Bellmann, E.; Shaheen, S. E.; Grubbs, R. H.; Marder, S. R.; Kippelen, B.; Peyghambarian, N. *Chem. Mater.* **1999**, *11*, 399. (b) Shaheen, S. E.; Jabbour, G. E.; Kippelen, B.; Peyghambarian, N.; Anderson, J. D.; Marder, S. R.; Armstrong, N. R.; Bellmann, E.; Grubbs, R. H. *Appl. Phys. Lett.* **1999**, *74*, 3212.

(8) (a) Smith, P. F.; Gerroir, P.; Xie, S.; Hor, A. M.; Popovic, Z. *Langmuir* **1998**, *14*, 5946. (b) Fenter, P.; Schreiber, F.; Bulović, V.; Forrest, S. R. *Chem. Phys. Lett.* **1997**, *277*, 521.

(9) (a) Ji, J.; Narayan-Sarathy, S.; Neilson, R. H.; Oxley, J. D.; Babb, D. A.; Rondon, N. G.; Smith, D. W., Jr. *Organometallic* **1998**, *17*, 783. (b) Smith, D. W., Jr.; Babb, D. A. *Marcomolecules* **1996**, *29*, 852.

(10) (a) Cao, Y.; Yu, G.; Zhang, C.; Menon, R.; Heeger, A. J. *Synth. Met.* **1997**, *87*, 171. (b) Berntsen, A.; Croonen, Y.; Liedenbaum, C.; Schoo, H.; Visser, R.-J.; Vleggaar, J.; van de Weijer, P. *Opt. Mater.* **1998**, *9*, 125.

(11) Choulis, S. A.; Choong, V.-E.; Mathai, M. K.; So, F. *Appl. Phys. Lett.* **2005**, *87*, 113503.

(12) (a) Elschner, A.; Bruder, F.; Heuer, H. W.; Jonas, F.; Karbach, A.; Kirchmeyer, S.; Thurm, S. *Synth. Met.* **2000**, *111*, 139. (b) Brown, T. M.; Kim, J. S.; Friend, R. H.; Cacialli, F.; Daik, R.; Feast, W. J. *Appl. Phys. Lett.* **1999**, *75*, 1679.

(13) Kim, J.-S.; Friend, R. H.; Grizzi, L.; Burroughes, J. H. *Appl. Phys. Lett.* **2005**, *87*, 023506.

(14) (a) Morgado, J.; Friend, R. H.; Cacialli, F. *Appl. Phys. Lett.* **2002**, *80*, 2436. (b) Yan, H.; Scott, B. J.; Huang, Q.; Marks, T. J. *Adv. Mater.* **2004**, *16*, 1948.

(15) Greczynski, G.; Kugler, Th.; Salaneck, W. R. *Thin Solid Films* **1999**, *354*, 129.

(16) (a) de Jong, M. P.; van lJzendoom, L.; de Voigt, M. J. A. *Appl. Phys. Lett.* **2000**, *77*, 2255. (b) Lee, Y. J. *Synth. Met.* **2006**, *156*, 537. (c) Wong, K. W.; Yip, H. L.; Luo, Y.; Wong, K. Y.; Lau, W. M.; Low, K. H.; Chow, H. F.; Gao, Z. Q.; Yeung, W. L.; Chang, C. C. *Appl. Phys. Lett.* **2002**, *80*, 2788.

(17) (a) Khuong, K. S.; Jones, W. H.; Pryor, W. A.; Houk, K. N. *J. Am. Chem. Soc.* **2005**, *127*, 1265. (b) Mayo, F. *J. Am. Chem. Soc.* **1968**, *90*, 1289. (c) Chong, Y. K.; Rizzardo, E.; Solomon, D. H. *J. Am. Chem. Soc.* **1983**, *105*, 7761.

(18) (a) Klärner, G.; Lee, J.-I.; Lee, V. Y.; Chan, E.; Chen, J.-P.; Nelson, A.; Markiewicz, D.; Siemens, R.; Scott, J. C.; Miller, R. D. *Chem. Mater.* **1999**, *11*, 1800. (b) Sun, H.; Liu, Z.; Hu, Y.; Wang, L.; Ma, D.; Jing, X.; Wang, F. *J. Polym. Sci., Part A: Polym. Chem.* **2004**, *42*, 2124.

(19) (a) Tang, C. W.; VanSlyke, S. A. *Appl. Phys. Lett.* **1987**, *51*, 913. (b) Shirota, Y. *J. Mater. Chem.* **2000**, *10*, 1. (c) O'Brien, D. F.; Burrows, P. E.; Forrest, S. R.; Koene, B. E.; Loy, D. E.; Thompson, M. E. *Adv. Mater.* **1998**, *10*, 1108.

Table 1. Physical Properties of HTMs

HTMs	active HTM[a] (%)	T_c[b] (°C)	T_d[c] (°C)	T_g[d] (°C)	HOMO/LUMO[e] (eV)
1-TPD	63.6	170	350	160	−5.3/−2.5
1-NPD	66.6	170	360	188	−5.4/−2.7
2-TPD	75.3	170	361	186	−5.3/−2.5
2-NPD	77.6	170	371	211	−5.4/−2.7

[a] Molecular weight percentage of active TPD or NPD moieties in the molecule. [b] T_c is the lowest curing temperature to obtain complete solvent resistance determined by absorption spectra. [c] T_d is decomposition temperature determined by TGA at 5% weight loss. [d] T_g was determined by the second heating of DSC. [e] HOMO energy level was calculated by CV using ferrocene value of −4.8 eV below the vacuum level.

to serve as the linker and provide adequate flexibility for styryl groups to react in the solid state. In addition, hole transporting of these HTMs can be optimized by increasing the contents of TPD or NPD. 2-TPD and 2-NPD consist of two connecting diamine molecules, and two styryl groups were designed to improve the content of active hole-transporter (75.3 and 77.6 wt %) over 1-TPD and 1-NPD (63.6 and 66.6 wt %) that contain two styryl groups on a single diamine molecule (Table 1). VB-TPD that possesses only a single styryl and TPD moiety was also synthesized for comparison. Herein, we report the synthesis and characterization of TPD- and NPD-based thermally cross-linkable HTMs and their applications for light-emitting diodes.

Results and Discussion

Synthesis of Materials. The synthetic details for making these new materials are depicted in Schemes 2−4. In a sequential Hartwig−Buchwald palladium-catalyzed amination, aniline was first coupled with 4-bromotoluene to yield compound **1**, which was then allowed to react with 4,4′-dibromobiphenyl to afford **2**. Vilsmeier formylation of compound **2** with 1 equiv of phosphorous oxachloride ($POCl_3$) and *N*,*N*-dimethylformamide (DMF) furnished product **3a**, whereas using 2 equiv of $POCl_3$ and DMF yielded the product **3b**. Reduction of the aldehyde on **3** by sodium borohydride generated the hydroxyl compound **4**. Similarly, the Pd-catalyzed coupling of 1-naphthylamine with 4,4′-dibromobiphenyl afforded **5a**, which could be treated with compound **6** to yield compound **7**. Desilylation of the *tert*-butyldimethylsilyl (TBDMS) groups on **7** using tetrabutylammonium fluoride (TBAF) resulted in the NPD-based compound **8** (Scheme 2).

Pd-catalyzed C−N coupling of **5** with 1 equiv of **6** generated single-side reacted product **9**. Then 2 equiv of secondary amine **9** was coupled with di-iodo compound **10** to yield **11**, which was further deprotected with TBAF to afford the connected dimer **12** (Scheme 3).

Etherification of dihydroxy compounds **4**, **8**, and **12** with 4-vinylbenzyl chloride using NaH as base furnished the corresponding hole-transporting materials VB-TPD, 1-TPD, 1-NPD, 2-TPD, and 2-NPD containing 4-vinylbenzyl ether as the cross-linking group (Scheme 4).

Cross-Linking and Thermal Properties. All the HTMs synthesized are very soluble in common organic solvents, such as THF, dichloromethane, chlorobenzene, and toluene. They can be spin-coated (2000 rpm) from their corresponding dichloroethane solutions (0.5 wt %) onto ITO substrate followed by thermal cross-linking under argon. The resultant films are very transparent and absorb mainly in the UV region so it causes very little interference with the light generated from the device.

Solvent resistance of cross-linked films was investigated by monitoring the UV–vis spectra of HTMs before and after rinsing with chlorobenzene (a good solvent for both precursor monomers and emissive polymer). As shown in Figure 1, a robust film of 1-TPD could be obtained by curing it at 170 °C for 30 min. This was evident by its unchanged absorption spectra. Similar phenomena were observed for 2-TPD, 1-NPD, and 2-NPD.

Because both of the styryl moieties on the precursor monomer underwent thermally initiated radical polymerization at 170 °C, it resulted in a cross-linked film with good solvent resistance. Even when these HTMs were cured at only 150 °C for 30 min, more than 85% of the film is still remained after washing with chlorobenzene. This indicates that sufficient solvent resistance already exist even though the film was only cured at such a low temperature. Compared with the higher curing temperature required for PFCB-based HTMs (230 °C for 1–2 h), this low-temperature curing process significantly reduces the fabrication time and cost. Although VB-TPD also has the same high active material ratio (77.8 wt %) compared to 2-TPD, the single styryl group on TPD can only form a linear polymer which does not provide needed solvent resistance even after it was cured at 200 °C for 1 h.

The first scan of differential scanning calorimetry (DSC) for each HTM monomer is shown in Figure 2. Both 1-TPD and 2-NPD showed board exothermic peaks with a T_{max} around 150 °C which is the result of thermal cross-linking of styrene groups. This temperature is reasonably close to the curing temperature (170 °C) needed for generating complete solvent-resistant network. Interestingly, 2-TPD exhibited a clear glass transition temperature (T_g) at ∼60 °C, and 1-NPD showed a melting point at ∼65 °C, inducing lower onset temperature of exothermic cross-linking. After the initial heating cycle, high T_g (161–211 °C) was observed for each material during the second DSC heating, indicating that the resultant cross-linked networks are highly amorphous, which can reduce the tendency of crystallization and maintain long-term morphological stability of organic films (Figure 3 and Table 1). The degree of cross-linking of these films is highly dependent on the condition of thermal treatment. The higher temperature and longer time of heating will yield the film with higher degree of cross-linking which can be evidenced by the increased glass transition temperatures.

The decomposition temperature (T_d) of HTMs was determined by thermogravimetric analysis (TGA). The resulting cross-linked network of HTMs possess high T_d, ranging from 350 to 371 °C. It is noteworthy that NPD derivatives are more stable than its TPD analogues by 10 °C. Besides, the connected dimers 2-TPD and 2-NPD also are more stable than its corresponding mono 1-TPD and 1-NPD compounds, respectively (Table 1).

Electrochemical Properties. Electrochemical properties of these cross-linked materials cured at 180 °C for 30 min

Scheme 2. Synthetic Route

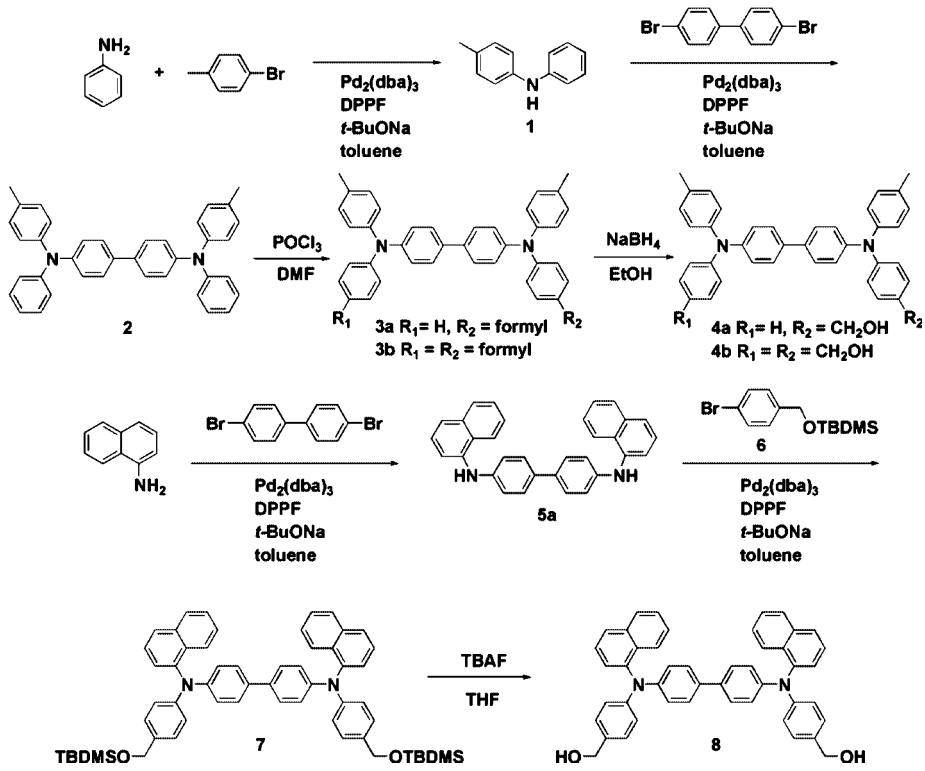

Scheme 3. Synthetic Route

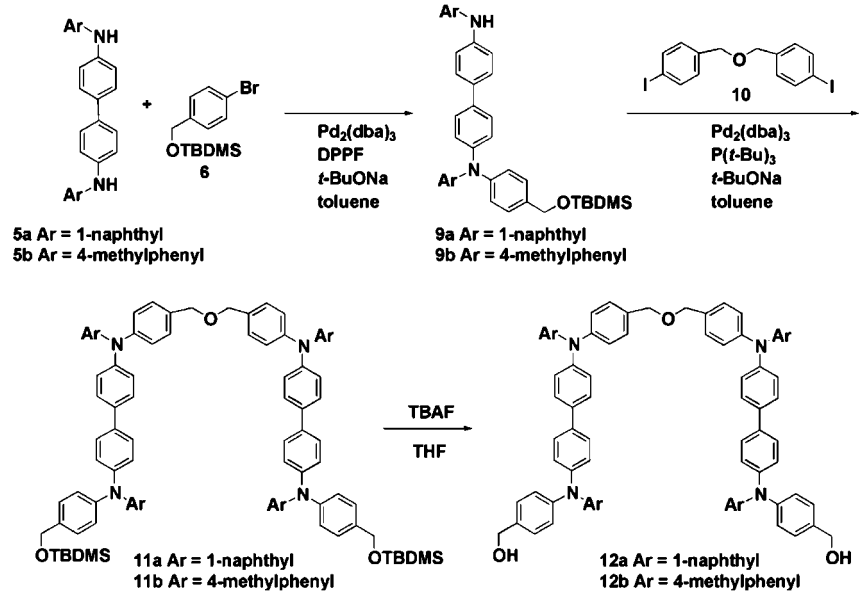

Scheme 4. Synthetic Route

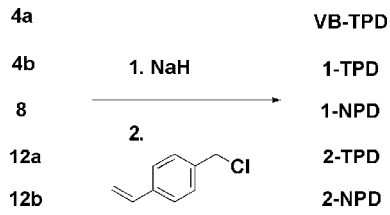

on ITO were investigated by cyclic voltammetry (CV). Notably, the first and second oxidative peaks in the anodic sweep for 1-TPD and 1-NPD are vaguely overlapped (Figure 4). However, for 2-TPD and 2-NPD, the two oxidative peaks could be distinguished clearly (Figure 5).

The CV curve for these cross-linked materials remained essentially unchanged (Figure 5) after 10 repetitive cycles, indicating excellent mechanical and electrochemical stability in these HTMs. However, it should be noted that VB-TPD after cured at 180 °C for 30 min exhibited relatively unstable CV curves and degraded significantly as the number of cycles increased, indicating single cross-linker on VB-TPD is not enough to warrant the robustness of HTM layer on ITO.

The highest occupied molecular orbital (HOMO) energy levels of these HTMs were estimated from the onset of oxidation potential using ferrocene/ferrocenium as standard,[20] while the lowest unoccupied molecular orbital (LUMO)

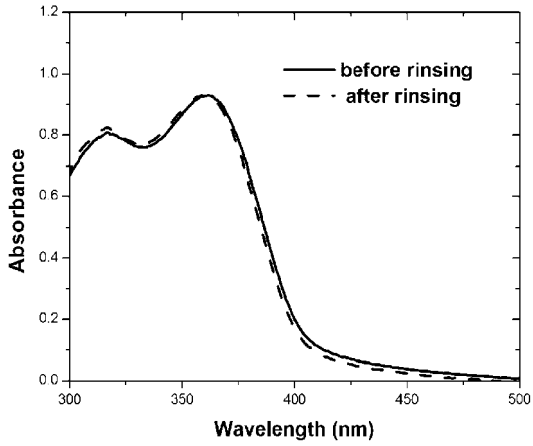

Figure 1. Absorption spectra of 1-TPD cured at 170 °C for 30 min, before washing (solid line) and after washing (dashed line) by chlorobenzene.

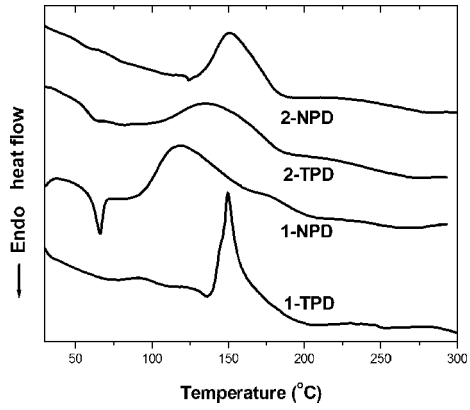

Figure 2. First heating of DSC measurements with a ramping rate of 10 °C/min.

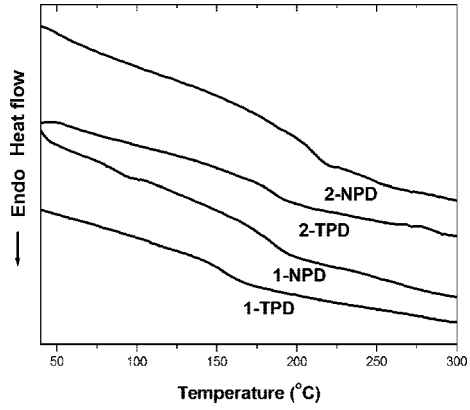

Figure 3. Second heating of DSC measurements with a ramping rate of 10 °C/ min.

levels were estimated from the difference between the HOMO energy level and the optical band gap measured from absorption spectrum (Table 1). Because the naphthyl group tends to lower the electron density of amine due to better electron delocalization, the HOMO of 1-NPD and 2-NPD (ca. −5.4 eV) is slightly higher than that of 1-TPD and 2-TPD (ca. −5.3 eV). These values are very close to the work function of ITO.

Atomic Force Microscopy (AFM) Images. The surface roughness of HTMs spin-coated and cross-linked on ITO

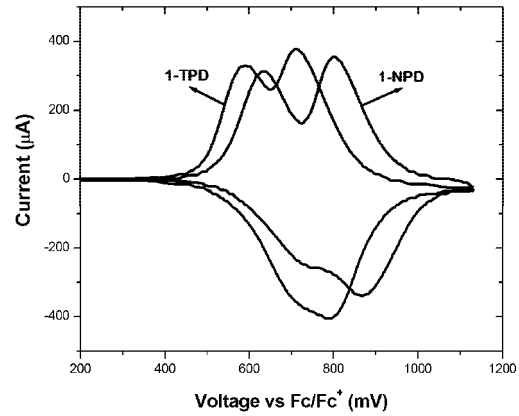

Figure 4. Cyclic voltammogram of cross-linked 1-TPD and 1-NPD films on ITO in a solution of n-Bu_4NPF_6 in acetonitrile (0.1 M) at a scan rate of 50 mV s^{-1}.

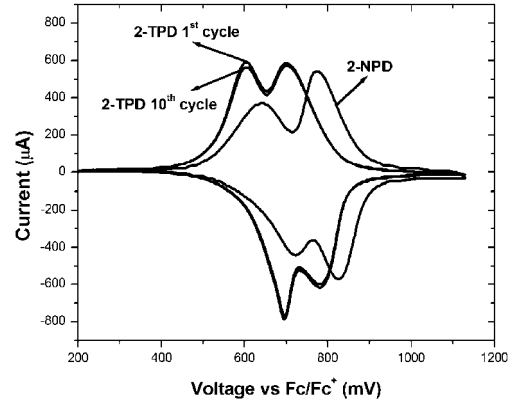

Figure 5. Cyclic voltammograms of cross-linked 2-TPD (1st cycle and 10th cycle are shown) and 2-NPD films on ITO in a solution of n-Bu_4NPF_6 in acetonitrile (0.1 M) at a scan rate of 50 mV s^{-1}.

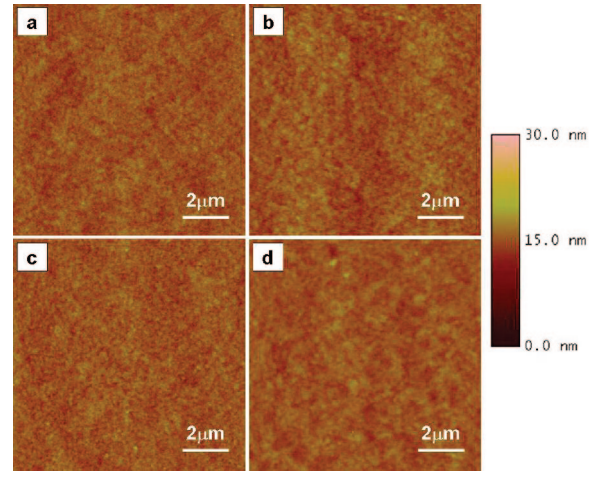

Figure 6. Atomic force microscopy images of HTMs spin-coated and cured on ITO: (a) 1-TPD rms roughness = 0.91 nm, (b) 2-TPD rms roughness = 0.88 nm, (c) 1-NPD rms roughness = 0.90 nm, and (d) 2-NPD rms roughness = 0.81 nm.

was examined by AFM (Figure 6). Polymerization in bulk often induces material shrinkage and results in microcracks in the films. Uniform film with no observable cracks or pinholes could be observed for each sample over a 10 × 10 mm scan area, and the root-mean-square (rms) surface roughness for 1-TPD, 2-TPD, 1-NPD, and 2-NPD is 0.91, 0.88, 0.90, and 0.81 nm, respectively. This shows that these

Scheme 5. PFBT5 Emissive Layer

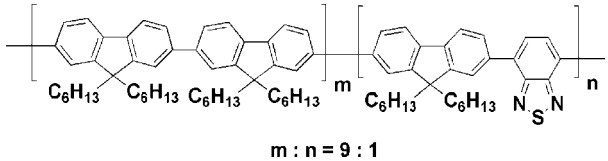

m : n = 9 : 1

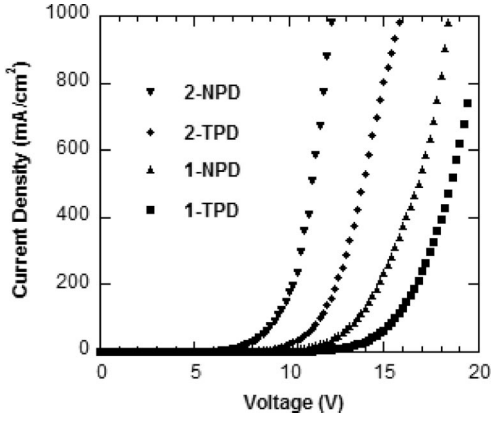

Figure 7. Current density–voltage ($J-V$) characteristics based on devices ITO/HTL/PFBT5/CsF/Al.

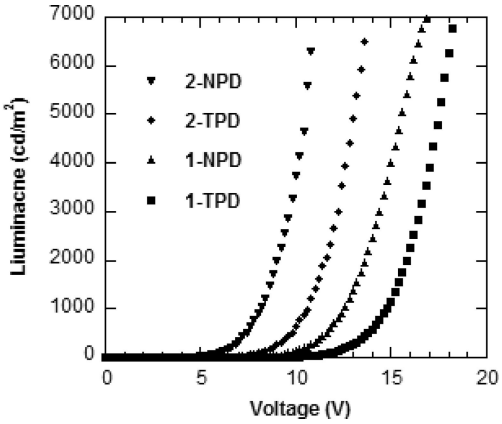

Figure 8. Luminance−voltage ($L-V$) characteristics based on devices ITO/HTL/PFBT5/CsF/Al.

cured HTMs provide another function of smoothing the rough surface of ITO which is usually with an rms roughness of ~3 nm.

Device Performance. LED devices with the configuration of ITO/HTL/PFBT5/CsF/Al were fabricated for evaluating the hole-transporting properties of these new materials. A fluorene-based poly[2,7-(9,9′-dihexylfluorene)-*co*-4,7-(2,1,3-benzothiadiazole)] denoted by PFBT5 was chosen as the green emitting layer[21] (Scheme 5).

The current density–voltage ($J-V$) and luminance−voltage ($L-V$) characteristics of the device are shown in Figure 7, Figure 8, and Table 2. As can be seen from Table 2, the device with 2-TPD as the HTL yielded a dramatic improved performance compared to the device made from 1-TPD. The same trend could also be observed in the 2-NPD and 1-NPD pair.

Table 2. Electroluminescence Data of Devices Based on the Structure ITO/HTL/PFBT5/CsF/Al

HTL[a]	V_{on}[b] (V)	Q_{max}[c] (%)	LE_{max}[d] (cd/A)	η_E[e] (lm/W)	B_{max}[f] (cd/m^2)	$V_{B_{max}}$[g] (V)
1-TPD	8.2	1.08	3.68	1.12	7780	18.6
1-NPD	7.8	1.64	5.60	1.85	11900	19.2
2-TPD	6.2	1.62	5.37	2.47	11600	17.2
2-NPD	4.6	1.89	6.21	3.87	13600	12.6

[a] Cross-linked at 180 °C for 30 min. [b] Turn-on voltage. [c] Maximum external quantum efficiency. [d] Maximum luminous efficiency. [e] Maximum power efficiency. [f] Maximum brightness. [g] Driving voltage corresponding to maximum brightness.

These results can be rationalized by the fact that 2-TPD and 2-NPD contain a higher ratio of active triarylamine components. This leads to better hole-transporting properties which significantly lowers the turn-on voltage and improves the overall device performance. Another reason for such device enhancement is the closer distance between the diamine moieties in 2-TPD and 2-NPD facilitates hole transport in cross-linked networks. Device based on 2-NPD as HTL exhibited the highest performance in terms of the turn-on voltage (4.6 V), external quantum efficiency (1.89%), luminous efficiency (6.21 cd/A), and maximum brightness (13 600 cd/m^2 at 12.6 V). In addition, the NPD-based materials showed better hole-transporting properties compared to their TPD-based analogues, as indicated by the lower turn-on voltages and concomitant increases in other device parameters. The similar observation can also be found for organic LEDs based on small molecule TPD and α-NPD.[22]

In order to realize the benefit of lower curing temperature in these HTMs, PEDOT:PSS was used as the bottom hole-injecting layer in the device configuration of ITO/PEDOT:PSS/HTL/PFBT5/CsF/Al to achieve optimal performance. The second hole-transporting layer was spin-coated and cross-linked on top of the PEDOT:PSS at 180 °C for 30 min. We then examined the morphology of the cured 2-NPD film by AFM. A very smooth film with a root-mean-square (rms) surface roughness of 0.68 nm was achieved, which is better than the corresponding film directly spun and cured on ITO with the rms roughness of 0.81 nm. However, it should be noted that when the 2-NPD film was cured at 230 °C for 30 min on top of ITO/PEDOT:PSS, the surface became rougher with an rms roughness of 0.85 nm. Figure 9 shows that all the devices showed uniform and stable emission with a λ_{max} at 540 nm from PFBT5, indicating that charge recombination occurs exclusively in the emissive layer.

Indeed, considerable enhancement of device performance could be achieved for each material. The luminous efficiency as a function of current density and device characteristics are shown in Figure 10 and Table 3. Again, devices using 2-TPD and 2-NPD as HTM showed better results than their corresponding counterparts, 1-TPD and 1-NPD. 2-NPD still exhibited the best device performance with a turn-on voltage of 3.3 V, maximum external quantum efficiency of 3.2%, luminous efficiency of 10.8 cd/A, and brightness of 21 500 cd/m^2. The control device using 2-NPD as the HTL but with the curing temperature increased to 230 °C for 30 min on

(20) (a) Pommerehne, J.; Vestweber, H.; Guss, W.; Mahrt, R. F.; Bassler, H.; Porsch, M.; Daub, J. *Adv. Mater.* **1995**, *7*, 551. (b) Liu, Y. Q.; Ma, H.; Jen, A. K.-Y. *Chem. Mater.* **1999**, *11*, 27.
(21) Herguth, P.; Jiang, X.; Liu, M. S.; Jen, A. K.-Y. *Macromolecules* **2002**, *35*, 6094.
(22) Kido, J.; Lizumi, Y. *Appl. Phys. Lett.* **1998**, *73*, 2721.

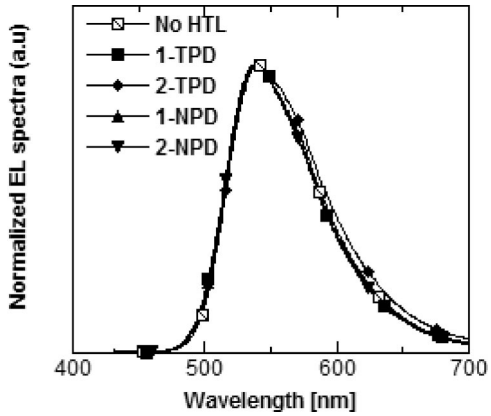

Figure 9. Electroluminescence based on the devices ITO/PEDOT:PSS/HTL/PFBT5/CsF/Al.

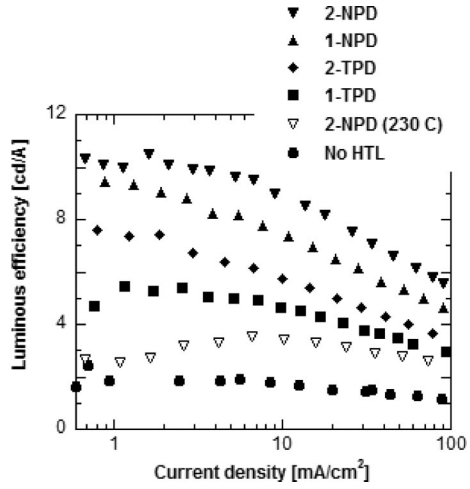

Figure 10. Luminous efficiency−current density relationship based on devices ITO/PEDOT:PSS/HTL/PFBT5/CsF/Al.

Table 3. Electroluminescence of Devices Based on the Structure ITO/PEDOT:PSS/HTL/PFBT5/CsF/Al

HTL	V_{on}[c] (V)	Q_{max}[d] (%)	LE_{max}[e] (cd/A)	η_E[f] (lm/W)	B_{max}[g] (cd/m^2)	$V_{B_{max}}$[h] (V)
Non	6.0	0.72	2.42	1.36	8180	14.6
1-TPD[a]	4.5	1.78	6.29	4.39	14200	14.2
1-NPD[a]	3.6	2.92	9.45	6.75	19500	11.8
2-TPD[a]	4.3	2.15	7.56	5.09	15800	12.5
2-NPD[a]	3.3	3.20	10.8	7.01	21500	12.1
2-NPD[b]	4.9	0.99	3.51	1.91	10400	12.2

[a] Cross-linked at 180 °C for 30 min. [b] Cross-linked at 230 °C for 30 min. [c] Turn-on voltage. [d] Maximum external quantum efficiency. [e] Maximum luminous efficiency. [f] Maximum power efficiency. [g] Maximum brightness. [h] Driving voltage corresponding to maximum brightness.

top of PEDOT:PSS was fabricated for parallel comparison. In a sharp contrast, the performance of this device dropped significantly. The maximum luminous efficiency of this device (3.51 cd/A) is approximately a factor of 3 lower than that of the device with 2-NPD cured at 180 °C and is 1.8 times lower than the device without PEDOT:PSS. This result shows that PEDOT:PSS can tolerate thermal treatment at 180 °C and improve device performance. However, a certain degree of degradation of PEDOT:PSS or acid-induced damage on ITO surface may occur upon heating at 230 °C, which is the temperature generally used for curing PFCB-typed HTMs.

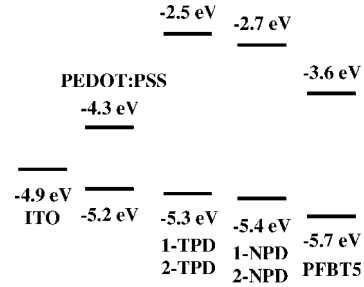

Figure 11. Energy level diagram of the materials in this research.

More notably, the device without using HTL layer gave rise to much poorer performances with higher turn-on voltage of 6 V and a maximum external quantum efficiency of only 0.72% (Table 3). The luminous efficiency of the device with bilayer PEDOT:PSS/1-NPD is ∼4 times higher than that of the device using single PEDOT:PSS layer. These results suggest that these TPD- and NPD-based triarylamine HTMs possess effective electron-blocking abilities at HTL/PFBT5 interface as a result of the large barrier ∼1 eV between the respective LUMO levels (Figure 11). This also reflects that electron-blocking ability of PEDOT:PSS is much weaker than that of diamine-based HTMs in terms of low-lying LUMO level of PEDOT:PSS.

In addition, it has been reported by Greenham et al. that the accumulation of electrons at the HTL/EML interface facilitates hole injection at lower fields and lowers the turn-on voltages.[23] Without these hole-transporting layers, however, electrons can easily overflow from PFBT5 through very conductive PEDOT:PSS to ITO anode, resulting in poor exciton recombination and hence lower the luminous efficiency of device. Furthermore, the separation of PEDOT:PSS and PFBT5 by inserting a layer of cross-linked HTM may prevent the emission quenching induced by the neighboring PEDOT:PSS layer due to its acidic nature. The TPD and NPD layers have the HOMO levels roughly at −5.3 and −5.4 eV, respectively, which are in between those of PEDOT:PSS (−5.2 eV) and PFBT5 (−5.7 eV). Therefore, the HTMs not only serve as the electron blocker but also provide an energy-matched cascade hole-injecting/transporting pathway which allows for more balanced charge carriers in the devices. The device performance can be further improved by introducing an electron-transporting layer to the device. The optimized results will be described in detail elsewhere. Although the cross-linking temperature of 180 °C was used in current study, a lower curing temperature is achievable based on the fact that over 85% of solvent resistance could be obtained by curing the films at 150 °C. Further study of curing temperature and curing time on the device performance is being pursued.

Conclusion

A new class of TPD- and NPD-based HTMs functionalized with the styryl group as the thermal cross-linkers have been rationally designed and synthesized. *In-situ* cross-linking of

(23) (a) Murata, K.; Cinà, S.; Greenham, N. C. *Appl. Phys. Lett.* **2001**, *79*, 1193. (b) Chi, J.; Huang, Q.; Veinot, J. G. C.; Yan, H.; Marks, T. J. *Adv. Mater.* **2002**, *14*, 565.

these HTMs was carried out by heating the thin films at 180 °C for 30 min to achieve robust, smooth, and solvent-resistant networks which are suitable for subsequent spin-coating of the emissive layer. In general, the NPD-based materials showed better performance in devices compared to their TPD-based analogues. The closely connected 2-NPD, which has the highest number density of active component, shows the best hole-transporting ability. The much milder cross-linking condition enables conducting polymer PEDOT:PSS to be inserted as the bottom hole-injection layer for fabricating multilayer devices. As a result, devices with a bilayer hole-injection/transport PEDOT:PSS/HTL/PFBT5 configuration can be fabricated by using all solution-processed materials to achieve significantly enhanced performance compared to those devices using only single-layer PEDOT:PSS/PFBT5 or HTL/PFBT5 configuration. Depending on the device requirements, the strategy of using styrene as an efficient cross-linker can also be integrated with various HTMs with different properties for realizing high power efficiency white PLED.[4h]

Experimental Section

General Measurement and Characterization. All chemicals are purchased from Aldrich as received unless otherwise specified. ^{1}H and ^{13}C NMR spectra were measured using Bruker 300 and 500 instrument spectrometers. High-resolution mass spectrometry (HRMS) was performed by the UW Bio Mass Spectrometry Laboratory. UV–vis absorption spectra were measured using a Perkin-Elmer Lambda 9 UV/vis/NIR spectrophotometer. Thermal transitions were measured on TA Instruments differential scanning calorimeter (DSC) 2010 and thermogravimetric analysis (TGA) 2950 under a nitrogen atmosphere at a heating rate of 10 °C/min. Cyclic voltammetric data were performed on a BAS CV-50W voltammetric analyzer using a conventional three-electrode cell with an ITO glass as the working electrode, a Pt gauze as the counter electrode, and an $Ag/AgNO_3$ as the reference electrode. 0.1 M tetrabutylammonium hexafluorophosphate ($TBAPF_6$) in acetonitrile is the electrolyte, and CV curves were calibrated using ferrocence as the standard, whose HOMO is −4.8 eV with respect to zero vacuum level. Atomic force microscopy (AFM, NanoScope III, Digital Instrument) equipped with an integrated silicon tip/cantilever with resonance frequency ∼240 kHz in height and phase image models were utilized for observation of morphologies. The AFM topographies showed no evidence of tip-induced modification during successive scans.

PLED Device Fabrication and Characterization. The PLEDs were fabricated on precleaned and O_2 plasma-treated ITO-covered glass substrates. After the plasma treatment, the substrates were moved into a glovebox, and all the subsequent film-forming processes were performed in it under argon protection. PEDOT:PSS (Bayer, AG) was spin-coated on ITO. HTLs were formed by spin-coating (2000 rpm) the corresponding HTM solutions (0.5 wt % in dichloroethane) onto ITO or on top of PEDOT:PSS and then thermally cross-linked on a hot plate at 180 °C for 30 min. Under this condition, we can generally obtain hole-transporting layers with ca. 25 nm thickness after cross-linking. EM in chlorobenzene was then spin-coated on top of the HTL(s). Cesium fluoride (CsF) with the thickness of 1 nm and Al (200 nm) were evaporated subsequently as cathode. The thickness of each layer in two device configurations is shown as the following: (1) ITO/HTL(∼25 nm)/PFBT5(∼65 nm)/CsF/Al; (2) ITO/PEDOT:PSS(∼40 nm)/HTL(∼25 nm)/PFBT5(∼65 nm)/CsF/Al. The performance testing was carried out at room temperature in air without encapsulation. Current density–voltage ($J-V$) characteristics of the devices were measured on a Hewlett-Packard 4155B semiconductor parameter analyzer. The EL spectra were recorded by a spectrometer (Instaspec IV, Oriel Co.). The light power of the EL emission was measured using a calibrated Si photodiode and a Newport 2835-C multifunctional optical meter. Photometric units (cd/m^2) were calculated using the forward output power together with the EL spectra of the devices under assumption of the emission's Lambertian space distribution.

Synthesis of Compound 3a. To a solution of **2** (3 g, 5.8 mmol) and DMF (0.5 mL, 5.8 mmol) in 1,2-dichloroethane (20 mL) was added $POCl_3$ (0.54 mL, 5.8 mmol) by syringe. The mixture was stirred at 90 °C for 24 h. After being cooled to room temperature (rt), the solution was poured into NaOAc solution (1 g in 50 mL) and stirred for 30 min. The mixture was extracted with CH_2Cl_2 and water. After the removal of organic solvent, the residue was directly purified by column chromatography on silica gel (hexane/ethyl acetate, v/v, 5/1) to obtain product **3a** (1.3 g, 40%). ^{1}H NMR (500 MHz, $CDCl_3$): δ 2.37 (s, 3 H), 2.41 (s, 3 H), 7.03–7.11 (m, 5 H), 7.12–7.18 (m, 8 H), 7.22 (d, J = 9.5 Hz, 2 H), 7.24 (d, J = 8.5 Hz, 2 H), 7.28 (d, J = 8 Hz, 1 H), 7.30 (d, J = 8 Hz, 1 H), 7.47 (d, J = 8.5 Hz, 2 H), 7.55 (d, J = 8.5 Hz, 2 H), 7.72 (d, J = 8.5 Hz, 2 H), 9.84 (s, 1 H). ^{13}C NMR (125 MHz, $CDCl_3$): δ 20.9, 21.0, 118.8, 122.5, 123.1, 123.8, 125.1, 126.0, 126.5, 127.3, 127.6, 128.6, 129.1, 130.0, 130.4, 131.3, 133.0, 133.5, 135.2, 137.0, 143.3, 144.7, 144.8, 147.2, 147.6, 153.3, 190.5. HRMS (ESI) (M^+, $C_{39}H_{32}N_2O$): calcd: 544.2515; found: 544.2518.

Synthesis of Compound 3b. To a solution of **2** (2.58 g, 5 mmol) and DMF (0.88 mL, 11.4 mmol) in 1,2-dichloroethane (20 mL) was added $POCl_3$ (1.1 mL, 11.8 mmol) by syringe. The mixture was stirred at 90 °C for 13 h. After being cooled to rt, the solution was poured into NaOAc solution (1 g in 50 mL) and stirred for 30 min. The mixture was extracted with CH_2Cl_2 and water. After the removal of organic solvent, the residue was directly purified by column chromatography on silica gel (hexane/ethyl acetate, v/v, from 8/1 to 6/1 then 4/1) to obtain product **3b** (1.9 g, 66%). ^{1}H NMR (500 MHz, $CDCl_3$): δ 2.40 (s, 6 H), 7.09 (d, J = 8.5 Hz, 2 H), 7.14 (d, J = 8.5 Hz, 2 H), 7.22 (d, J = 8.5 Hz, 2 H), 7.25 (d, J = 8.5 Hz, 2 H), 7.55 (d, J = 8.5 Hz, 2 H), 7.72 (d, J = 8.5 Hz, 2 H), 9.84 (s, 1 H). ^{13}C NMR (125 MHz, $CDCl_3$): δ 21.0, 119.1, 125.9, 126.6, 127.8, 128.7, 130.4, 131.3, 135.3, 136.4, 143.2, 145.2, 153.2, 190.5. HRMS (ESI) (M^+, $C_{40}H_{32}N_2O_2$): calcd: 572.2464; found: 572.2458.

Synthesis of Compound 4a. To a solution of **3a** (1.2 g, 2.2 mmol) in EtOH (50 mL) was added $NaBH_4$ (0.33 g, 8.8 mmol). The mixture was refluxed under N_2 for 18 h. Water was added carefully to quench the reaction. After the removal of EtOH, the residue was directly purified by column chromatography on silica gel (hexane/ethyl acetate, v/v, 2.5/1) to obtain product **4a** (0.98 g, 81%). ^{1}H NMR (500 MHz, $CDCl_3$): δ 2.39 (s, 6 H), 4.67 (s, 2 H), 7.03–7.19 (m, 17 H), 7.27–7.33 (m, 4 H), 7.47 (d, J = 8 Hz, 4 H). ^{13}C NMR (125 MHz, $CDCl_3$): δ 20.8, 21.1, 64.9, 122.3, 123.39, 123.44, 123.5, 123.6, 124.9, 127.1, 127.1, 128.2, 129.1, 129.88, 129.91, 132.8, 132.9, 134.1, 134.4, 134.5, 144.8, 144.9, 146.5, 146.7, 147.3, 147.7. HRMS (ESI) (M^+, $C_{39}H_{34}N_2O$): calcd: 546.2671; found: 546.2665.

Synthesis of Compound 4b. To a solution of **3b** (1.8 g, 3.15 mmol) in EtOH (100 mL) was added $NaBH_4$ (0.95 g, 25.2 mmol). The mixture was refluxed under N_2 for 18 h. Water was added carefully to quench the reaction. After the removal of EtOH, the residue was directly purified by column chromatography on silica gel (hexane/ethyl acetate, v/v, 1/1) to obtain product **4b** (1.6 g, 88%). ^{1}H NMR (500 MHz, $CDCl_3$): δ 2.36 (s, 6 H), 4.64 (s, 4 H), 7.06 (d, J = 8.5 Hz, 2 H), 7.09–7.14 (m, 12 H), 7.26 (d, J = 8.5

Hz, 2 H), 7.43 (d, $J = 9$ Hz, 2 H). ^{13}C NMR (125 MHz, $CDCl_3$): δ 20.8, 64.9, 123.4, 123.5, 124.9, 127.1, 128.2, 129.9, 132.9, 134.3, 134.5, 144.3, 146.6, 147.3. HRMS (ESI) (M^+, $C_{40}H_{36}N_2O_2$): calcd: 576.2777; found: 576.2783.

Synthesis of Compound VB-TPD. To a solution of **4a** (0.8 g, 1.46 mmol) in dry DMF (5 mL) was added NaH (53 mg, 2.2 mmol). The mixture was stirred at room temperature for 1 h. 4-Vinylbenzyl chloride (0.25 mL, 1.75 mmol) was added to above solution by syringe. The mixture was heated at 60 °C for 24 h. Water was added to quench the reaction. The organic solvent was extracted with CH_2Cl_2 and water to remove DMF. After the removal of CH_2Cl_2, the residue was directly purified by column chromatography on silica gel (hexane/ethyl acetate, v/v, 9/1) to give a solid VB-TPD (0.62 g, 64%). ^{1}H NMR (500 MHz, $CDCl_3$): δ 2.39 (s, 6 H), 4.54 (s, 2 H), 4.64 (s, 2 H), 5.31 (d, $J = 10.5$ Hz, 1 H), 5.83 (d, $J = 17.5$ Hz, 1 H), 6.78 (dd, $J_1 = 10.5$ Hz, $J_2 = 17.5$ Hz, 1 H), 7.05 (dd, $J_1 = 7$ Hz, $J_2 = 7.5$ Hz, 1 H), 7.08–7.19 (m, 16 H), 7.27–7.33 (m, 4 H), 7.41 (d, $J = 8$ Hz, 2 H), 7.48 (d, $J = 8.5$ Hz, 6 H). ^{13}C NMR (125 MHz, $CDCl_3$): δ 20.9, 71.7, 71.8, 113.8, 122.3, 123.41, 123.42, 123.5, 123.6, 124.9, 126.2, 127.1, 128.0, 129.05, 129.10, 129.9, 131.8, 132.8, 132.9, 134.2, 134.3, 136.4, 136.8, 137.8, 144.4, 145.0, 146.6, 146.7, 147.3, 147.7. HRMS (ESI) (M^+, $C_{48}H_{42}N_2O$): calcd: 662.3297; found: 662.3288.

Synthesis of Compound 1-TPD. To a solution of **4b** (0.8 g, 1.39 mmol) in dry DMF (10 mL) was added NaH (0.1 g, 4.17 mmol). The mixture was stirred at room temperature for 1 h and then cooled to 0 °C. 4-Vinylbenzyl chloride (0.47 mL, 3.3 mmol) was added to above solution by syringe. The mixture was heated at 60 °C for 24 h. Water was added to quench the reaction. The organic solvent was extracted with CH_2Cl_2 and water to remove DMF. After the removal of CH_2Cl_2, the residue was directly purified by column chromatography on silica gel (hexane/ethyl acetate, v/v, 8/1) to give a solid 1-TPD (0.6 g, 54%). ^{1}H NMR (300 MHz, $CDCl_3$): δ 2.35 (s, 6 H), 4.51 (s, 4 H), 4.60 (s, 4 H), 5.27 (d, $J = 10.8$ Hz, 2 H), 5.77 (d, $J = 17.4$ Hz, 2 H), 6.75 (dd, $J_1 = 10.8$ Hz, $J_2 = 17.4$ Hz, 2 H), 7.0–7.2 (m, 16 H), 7.2–7.3 (m, 3 H), 7.3–7.5 (m, 13 H). ^{13}C NMR (125 MHz, $CDCl_3$): δ 20.8, 71.8, 71.9, 113.8, 123.5, 123.6, 125.0, 126.2, 127.2, 128.0, 129.0, 130.0, 132.0, 132.9, 134.4, 136.6, 137.0, 138.0, 145.0, 146.8, 147.4. HRMS (ESI) (M^+, $C_{58}H_{52}N_2O_2$): calcd: 808.4029; found: 808.4036.

Synthesis of Compound 7. A solution of **5a** (2.5 g, 5.73 mmol), **6** (3.8 g, 12.6 mmol), $Pd_2(dba)_3$ (0.19 g, 0.2 mmol), 1,1′-bis(diphenylphosphino)ferrocene (0.17 g, 0.3 mmol), and *t*-BuONa (1.8 g, 18.7 mmol) in toluene (100 mL) was stirred at 110 °C for 24 h. The solvent was removed in vacuo, and the residue was purified by column chromatography on silica gel (hexane/ethyl acetate, v/v, 9/1) to give a solid **7** (2.3 g, 46%). ^{1}H NMR (500 MHz, $CDCl_3$): δ 0.16 (s, 12 H), 0.98 (s, 18 H), 4.74 (s, 4 H), 7.08 (d, $J = 8$ Hz, 4 H), 7.10 (d, $J = 8.5$ Hz, 4 H), 7.23 (d, $J = 8.5$ Hz, 4 H), 7.39 (d, $J = 7.5$ Hz, 4 H), 7.42 (d, $J = 8.5$ Hz, 4 H), 7.49 (d, $J = 7.5$ Hz, 2 H), 7.52 (d, $J = 7.5$ Hz, 2 H), 7.82 (d, $J = 8$ Hz, 2 H), 7.93 (d, $J = 8.5$ Hz, 2 H), 8.01 (d, $J = 8.5$ Hz, 2 H). ^{13}C NMR (125 MHz, $CDCl_3$): δ 18.4, 16.0, 64.8, 121.6, 122.0, 124.3, 126.1, 126.31, 126.34, 127.0, 127.09, 127.10, 128.3, 131.2, 133.6, 134.8, 135.3, 143.5, 147.2, 147.4. HRMS (ESI) (M^+, $C_{58}H_{64}N_2O_2Si_2$): calcd: 876.4506; found: 876.4514.

Synthesis of Compound 8. To a solution of **7** (2.4 g, 2.73 mmol) in THF (20 mL) was added 1 M solution of TBAF in THF (6 mL, 6 mmol). The mixture was stirred at room temperature for 2 h. After the removal of THF, the residue was purified by column chromatography on silica gel (hexane/ethyl acetate, v/v, 1/1 then 3/1) to give product **8** (1.6 g, 90%). ^{1}H NMR (500 MHz, $CDCl_3$): δ 4.61(s, 4 H), 7.09 (d, $J = 8.5$ Hz, 8 H), 7.23 (d, $J = 8.5$ Hz, 4 H), 7.34–7.44 (m, 8 H), 7.46–7.55 (m, 4 H), 7.81 (d, $J = 8.5$ Hz, 2 H), 7.93 (d, $J = 8.5$ Hz, 2 H), 7.99 (d, $J = 8.5$ Hz, 2 H). ^{13}C NMR (125 MHz, $CDCl_3$): δ 64.9, 121.8, 121.9, 124.1, 126.1, 126.3, 126.4, 126.5, 127.06, 127.11, 128.2, 128.4, 131.1, 133.8, 134.0, 135.2, 143.3, 147.1, 147.8. HRMS (ESI) (M^+, $C_{46}H_{36}N_2O_2$): calcd: 648.2777; found: 648.2778.

Synthesis of Compound 1-NPD. To a solution of **8** (0.75 g, 1.16 mmol) in dry DMF (8 mL) was added NaH (83.5 mg, 3.48 mmol). The mixture was stirred at room temperature for 1 h and then cooled to 0 °C. 4-Vinylbenzyl chloride (0.4 mL, 2.78 mmol) was added to above solution by syringe. The mixture was heated at 60 °C for 24 h. Water was added to quench the reaction. The organic solvent was extracted with CH_2Cl_2 and water to remove DMF. After the removal of CH_2Cl_2, the residue was directly purified by column chromatography on silica gel (hexane/ethyl acetate, v/v, 6/1 then 4/1) to give a solid 1-NPD (0.61 g, 60%). ^{1}H NMR (500 MHz, $CDCl_3$): δ 4.53 (s, 4 H), 4.63 (s, 4 H), 5.31 (d, $J = 10$ Hz, 2 H), 5.82 (d, $J = 17.5$ Hz, 2 H), 6.79 (dd, $J_1 = 10$ Hz, $J_2 = 17.5$ Hz, 2 H), 7.13 (s, br, 8 H), 7.27 (d, $J = 6$ Hz, 4 H), 7.35–7.65 (m, 20 H), 7.84 (d, $J = 6.5$ Hz, 2 H), 7.95 (d, $J = 6.5$ Hz, 2 H), 8.03 (d, $J = 7$ Hz, 2 H). ^{13}C NMR (125 MHz, $CDCl_3$): δ 71.8, 113.7, 121.7, 121.9, 124.2, 126.1, 126.2, 126.3, 126.4, 126.5, 127.0, 127.2, 127.9, 128.3, 129.0, 131.1, 131.3, 133.8, 135.2, 136.5, 136.9, 137.9, 143.3, 147.1, 147.8. HRMS (ESI) (M^+, $C_{64}H_{52}N_2O_2$): calcd: 880.4029; found: 880.4035.

Synthesis of Compound 9b. A solution of **5b** (2.9 g, 7.95 mmol), **6** (2.4 g, 7.95 mmol), $Pd_2(dba)_3$ (0.12 g, 0.13 mmol), 1,1′-bis(diphenylphosphino)ferrocene (0.14 g, 0.25 mmol), and *t*-BuONa (1 g, 10.4 mmol) in toluene (100 mL) was stirred at 110 °C for 24 h. The solvent was removed in vacuo, and the residue was purified by column chromatography on silica gel (hexane/ethyl acetate, v/v, 6/1) to give a solid **9b** (1.86 g, 40%). ^{1}H NMR (500 MHz, $CDCl_3$): δ 0.22 (s, 6 H), 1.06 (s, 9 H), 2.41 (s, 6 H), 4.80 (s, 2 H), 7.05–7.25 (m, 14 H), 7.31 (d, $J = 8$ Hz, 2 H), 7.51 (d, $J = 5.5$ Hz, 2 H), 7.54 (d, $J = 8$ Hz, 2 H). ^{13}C NMR (125 MHz, $CDCl_3$): δ −5.0, 18.4, 20.8, 26.0, 64.8, 117.1, 118.9, 123.0, 123.5, 123.8, 123.8, 124.7, 126.9, 127.1, 129.9, 132.5, 135.4, 145.2, 146.8. HRMS (ESI) (M^+, $C_{39}H_{44}N_2OSi$): calcd: 584.3223; found: 584.3229.

Synthesis of Compound 11b. $Pd_2(dba)_3$ (45.8 mg, 0.05 mmol) and tri-*tert*-butylphosphane (61 mg, 0.3 mmol) were dissolved under N_2 in dry toluene (15 mL). After being stirred for 10 min at room temperature, **9b** (1.3 g, 2.2 mmol), **10** (0.5 g, 1.1 mmol), and *t*-BuONa (0.25 g, 2.6 mmol) were added to the solution. The solution was degassed and with N_2 for 5 min and then was heated at 100 °C for 16 h. After being cooled to room temperature, the solvent was removed in vacuo and the residue was purified by column chromatography on silica gel (hexane/ethyl acetate, v/v, 8/1) to give a solid **11b** (0.9 g, 60%). ^{1}H NMR (500 MHz, $CDCl_3$): δ 0.17 (s, 12 H), 1.01 (s, 18 H), 2.38 (s, 12 H), 4.57 (s, 4 H), 4.76 (s, 4 H), 7.08 (d, $J = 3.5$ Hz, 4 H), 7.10 (d, $J = 3.5$ Hz, 4 H), 7.11–7.18 (m, 24 H), 7.26 (d, $J = 8$ Hz, 4 H), 7.30 (d, $J = 8.5$ Hz, 4 H), 7.46 (d, $J = 3.5$ Hz, 4 H), 7.47 (d, $J = 3.5$ Hz, 4 H). ^{13}C NMR (125 MHz, $CDCl_3$): δ −5.2, 18.4, 20.8, 26.0, 64.8, 72.0, 123.3, 123.5, 123.6, 123.9, 124.8, 125.0, 127.13, 127.14, 129.0, 129.89, 129.94, 132.2, 132.7, 132.9, 134.2, 134.5, 135.6, 145.1, 145.2, 146.71, 146.72, 147.0, 147.4. HRMS (ESI) (M^+, $C_{92}H_{98}N_4O_3Si_2$): calcd: 1362.7177; found: 1362.7168.

Synthesis of Compound 12b. To a solution of **11b** (0.85 g, 0.63 mmol) in THF (10 mL) was added 1 M solution of TBAF in THF (1.4 mL, 1.4 mmol). The mixture was stirred at room temperature for 10 h. After the removal of THF, the residue was purified by column chromatography on silica gel (hexane/ethyl acetate, v/v, 1/1) to give product **12b** (0.6 g, 84%). ^{1}H NMR (500 MHz, $CDCl_3$): δ 2.37 (s, 12 H), 4.57 (s, 4 H), 4.66 (s, 4 H), 7.06–7.11 (m, 8 H), 7.11–7.19 (m, 24 H), 7.28 (d, $J = 7$ Hz, 4 H), 7.30 (d, $J = 7.5$ Hz,

4 H), 7.46 (d, $J = 8$ Hz, 8 H). ^{13}C NMR (125 MHz, $CDCl_3$): δ 20.8, 25.6, 65.0, 71.4, 123.5, 123.5, 123.55, 123.60, 125.0, 127.15, 127.17, 128.2, 129.0, 129.9, 130.0, 132.1, 132.88, 132.93, 134.3, 134.5, 134.7, 144.97, 144.99, 146.7, 146.8, 147.4, 147.5. HRMS (ESI) (M^+, $C_{80}H_{70}N_4O_3$): calcd: 1134.5448; found: 1134.5443.

Synthesis of Compound 2-TPD. To a solution of **12b** (0.4 g, 0.35 mmol) in dry DMF (5 mL) was added NaH (25.2 mg, 1.05 mmol). The mixture was stirred at room temperature for 1 h and then cooled to 0 °C. 4-Vinylbenzyl chloride (0.12 mL, 0.84 mmol) was added to above solution by syringe. The mixture was heated at 60 °C for 24 h. Water was added to quench the reaction. The organic solvent was extracted with CH_2Cl_2 and water to remove DMF. After the removal of CH_2Cl_2, the residue was directly purified by column chromatography on silica gel (hexane/ethyl acetate, v/v, 5/1) to give a solid 2-TPD (0.34 g, 71%). ^{1}H NMR (500 MHz, $CDCl_3$): δ 2.37 (s, 12 H), 4.57 (s, 4 H), 4.53 (s, 4 H), 4.57 (s, 4 H), 4.62 (s, 4 H), 5.29 (d, $J = 11$ Hz, 2 H), 5.80 (d, $J = 17.5$ Hz, 4 H), 6.77 (dd, $J_1 = 11$ Hz, $J_2 = 17.5$ Hz, 2 H), 7.09 (d, $J = 8$ Hz, 8 H), 7.11–7.20 (m, 24 H), 7.26 (d, $J = 8.5$ Hz, 4 H), 7.30 (d, $J = 7.5$ Hz, 4 H), 7.47 (d, $J = 7.5$ Hz, 12 H). ^{13}C NMR (125 MHz, $CDCl_3$): δ 20.8, 71.8, 71.9, 72.0, 113.8, 123.49, 123.52, 123.57, 123.59, 125.0, 126.2, 127.2, 128.0, 129.01, 129.04, 129.9, 132.0, 132.2, 132.9, 134.41, 134.44, 136.5, 137.0, 138.0, 145.0, 146.75, 146.77, 147.41, 147.44. HRMS (ESI) (M^+, $C_{98}H_{86}N_4O_3$): calcd: 1366.6700; found: 1366. 6727.

Synthesis of Compound 9a. A solution of **5a** (2 g, 4.58 mmol), **6** (1.38 g, 4.58 mmol), $Pd_2(dba)_3$ (68 mg, 0.074 mmol), 1,1′-bis(diphenylphosphino)ferrocene (83 mg, 0.15 mmol), and *t*-BuONa (0.6 g, 6.2 mmol) in toluene (50 mL) was stirred at 110 °C for 24 h. The solvent was removed in vacuo, and the residue was purified by column chromatography on silica gel (hexane/ethyl acetate, v/v, 6/1) to give a solid **9a** (1.35 g, 45%). ^{1}H NMR (500 MHz, $CDCl_3$): δ 0.16 (s, 6 H), 1.00 (s, 9 H), 4.73 (s, 2 H), 6.02 (s, 1 H), 7.03–7.19 (m, 6 H), 7.23 (d, $J = 8$ Hz, 2 H), 7.37–7.59 (m, 12 H), 7.62 (d, $J = 5.5$ Hz, 1 H), 7.82 (d, $J = 8$ Hz, 1 H), 7.92 (d, $J = 8.5$ Hz, 1 H), 7.94 (d, $J = 8.5$ Hz, 1 H), 8.03 (d, $J = 8$ Hz, 1 H), 8.08 (d, $J = 8$ Hz, 1 H). ^{13}C NMR (125 MHz, $CDCl_3$): δ −5.1, 18.4, 26.0, 64.8, 115.9, 117.7, 121.7, 121.8, 122.0, 124.4, 125.7, 126.0, 126.1, 126.3, 126.4, 127.0, 127.1, 127.4, 127.7, 128.4, 128.5, 131.3, 133.0, 133.9, 134.7, 134.8, 135.3, 138.7, 143.6, 147.3, 147.3. HRMS (ESI) (M^+, $C_{45}H_{44}N_2OSi$): calcd: 656.3233; found: 656.3221.

Synthesis of Compound 11a. $Pd_2(dba)_3$ (23 mg, 0.025 mmol) and tri-*tert*-butylphosphane (30 mg, 0.15 mmol) were dissolved under N_2 in dry toluene (10 mL). After being stirred for 10 min at room temperature, **9a** (0.6 g, 0.9 mmol), **10** (0.2 g, 0.45 mmol), and *t*-BuONa (0.1 g, 1 0.04 mmol) were added to the solution. The solution was degassed and with N_2 for 5 min and then was heated at 100 °C for 16 h. After being cooled to room temperature, the solvent was removed in vacuo, and the residue was purified by column chromatography on silica gel (hexane/ethyl acetate, v/v, 6/1) to give a solid **11a** (0.4 g, 59%). ^{1}H NMR (500 MHz, $CDCl_3$): δ 0.17 (s, 12 H), 1.01 (s, 18 H), 4.53 (s, 4 H), 4.75 (s, 4 H), 7.04–7.14 (m, 16 H), 7.24 (d, $J = 8$ Hz, 4 H), 7.25 (d, $J = 8$ Hz, 4 H), 7.35–7.46 (m, 16 H), 7.46–7.56 (m, 8 H), 7.82 (d, $J = 8.5$ Hz, 4 H), 7.94 (d, $J = 6$ Hz, 4 H), 8.00 (d, $J = 8$ Hz, 2 H), 8.02 (d, $J = 8$ Hz, 2 H). ^{13}C NMR (125 MHz, $CDCl_3$): δ −5.2, 18.4, 26.0, 64.8, 71.9, 121.6, 121.7, 121.9, 122.0, 124.25, 124.33, 126.08, 126.11, 126.3, 126.35, 126.38, 126.5, 127.0, 127.1, 127.2, 128.3, 129.0, 131.2, 131.5, 133.5, 133.9, 134.9, 135.2, 143.4, 143.5, 147.1, 147.2, 147.4, 147.8. HRMS (ESI) (M^+, $C_{104}H_{98}N_4O_3Si_2$): calcd: 1506.7177; found: 1506.7167.

Synthesis of Compound 12a. To a solution of **11a** (0.4 g, 0.27 mmol) in THF (10 mL) was added 1 M solution of TBAF in THF (0.58 mL, 0.58 mmol). The mixture was stirred at room temperature for 3 h. After the removal of THF, the residue was purified by column chromatography on silica gel (hexane/ethyl acetate, v/v, 1/1) to give product **12a** (0.27 g, 80%). ^{1}H NMR (500 MHz, $CDCl_3$): δ 4.50 (s, 4 H), 4.64 (s, 4 H), 7.03–7.18 (m, 16 H), 7.22 (d, $J = 6.5$ Hz, 4 H), 7.24 (d, $J = 6.4$ Hz, 4 H), 7.35–7.45 (m, 16 H), 7.45–7.6 (m, 8 H), 7.80 (d, $J = 6.5$ Hz, 2 H), 7.81 (d, $J = 7$ Hz, 2 H), 7.91 (d, $J = 7$ Hz, 2 H), 7.92 (d, $J = 6.5$ Hz, 2 H), 7.95–8.2 (m, 4 H). ^{13}C NMR (125 MHz, $CDCl_3$): δ 65.0, 71.9, 121.7, 121.8, 121.9, 122.0, 124.16, 124.21, 126.10, 126.13, 126.3, 126.38, 126.41, 126.47, 126.51, 127.05, 127.08, 127.14, 127.15, 128.2, 128.35, 128.38, 129.0, 131.12, 131.13, 131.5, 133.7, 133.95, 133.98, 135.22, 135.24, 143.28, 143.30, 147.1, 147.2, 147.8, 147.9. HRMS (ESI) (M^+, $C_{92}H_{70}N_4O_3$): calcd: 1278.5448; found: 1278.5461.

Synthesis of Compound 2-NPD. To a solution of **12a** (0.22 g, 0.17 mmol) in dry DMF (8 mL) was added NaH (12.4 mg, 0.52 mmol). The mixture was stirred at room temperature for 1 h and then cooled to 0 °C. 4-Vinylbenzyl chloride (0.07 mL, 0.52 mmol) was added to above solution by syringe. The mixture was heated at 60 °C for 24 h. Water was added to quench the reaction. The organic solvent was extracted with CH_2Cl_2 and water to remove DMF. After the removal of CH_2Cl_2, the residue was directly purified by column chromatography on silica gel (hexane/CH_2Cl_2, v/v, 1/4) to give a solid 2-NPD (0.18 g, 70%). ^{1}H NMR (500 MHz, $CDCl_3$): δ 4.50 (s, 4 H), 4.51 (s, 4 H), 4.60 (s, 4 H), 5.28 (d, $J = 11$ Hz, 2 H), 5.79 (d, $J = 17.5$ Hz, 2 H), 6.76 (d, $J_1 = 11$ Hz, $J_2 = 17.5$ Hz, 2 H), 7.03–7.14 (m, 16 H), 7.23 (d, $J = 8$ Hz, 4 H), 7.24 (d, $J = 8$ Hz, 4 H), 7.35–7.46 (m, 24 H), 7.46–7.56 (m, 8 H), 7.805 (d, $J = 8$ Hz, 2 H), 7.813 (d, $J = 8$ Hz, 2 H), 7.91 (d, $J = 8$ Hz, 2 H), 7.92 (d, $J = 8$ Hz, 2 H), 7.97 (d, $J = 8$ Hz, 2 H), 7.98 (d, $J = 8$ Hz, 2 H). ^{13}C NMR (125 MHz, $CDCl_3$): δ 71.81, 71.84, 71.9, 113.7, 121.71, 121.7, 121.89, 121.94, 124.2, 126.2, 126.3, 126.4, 126.5, 127.1, 127.2, 128.0, 128.4, 129.01, 129.03, 130.0, 131.2, 131.3, 131.5, 133.8, 133.9, 135.3, 136.5, 136.9, 138.0, 143.4, 147.2, 147.2, 147.8, 147.9. HRMS (ESI) (M^+, $C_{110}H_{86}N_4O_3$): calcd: 1510.6700; found: 1510.6734.

Acknowledgment. This work was supported by the National Science Foundation (NSF-STC program under DMR-0120967) and the University of Washington through the Technology Gap Innovation Fund. Alex K.-Y. Jen thanks the Boeing-Johnson Foundation for its support.

CM071828O